Journal of Solid Mechanics Vol. 15, No. 4 (2023) pp. 449-468
DOI: 10.22034/jsm.2023.1987288.1778

Research Paper

An Analytical Study On Surface Energy Effect On Free Longitudinal Vibration of Cracked Nanorods

H. Shokrollahi [1,*], R. Nazemnezhad [2]

[1] *Department of Mechanical Engineering, Faculty of Engineering, Kharazmi University, Tehran, Iran*
[2] *School of Engineering, Damghan University, Damghan, Iran*

Received 19 June 2023; accepted 13 August 2023

ABSTRACT

The present work analytically studies the free longitudinal vibration of nanorods in the presence of cracks based on the surface elasticity theory. To this end, governing equations of motion and corresponding boundary conditions are obtained using Hamilton's principle. Due to considering the surface stress effect, as well as the surface density and the surface Lamé constants, the obtained governing equations of motion become non-homogeneous. The non-homogeneous governing equations are solved using appropriate analytical methods, and the natural frequencies are extracted. To have a comprehensive research, the effects of various parameters such as the length and radius of the nanorod, the crack severity, the crack position, the type of boundary condition, and the values of surface and bulk material properties on axial frequencies of the nanorod are investigated. Since this work considers the effects of all surface energy parameters, it can be claimed that it is a comprehensive study in this regard.

Keywords: Cracked nanorod; Longitudinal vibration; Surface energy.

1 INTRODUCTION

DEFECTS may establish/create intentionally or unintentionally in structures. Defects are created intentionally when a structure is designed in such a way that one element of the structure collapses instead of the entire structure in critical situations like earthquakes [1]. Therefore, the source of this type of defect is an engineering design. On the other hand, the defects created unintentionally may appear due to issues such as material, manufacturing processes, and operation. This kind of defect is almost always destructive. Therefore, it should be detected before causing serious damage to structures. One of these destructive defects is the crack which is very common in structures. The crack can appear in structures with macro-, micro-, or nano-scale.

[*] Corresponding author. Tel.: +98 21 88830891, Fax: +98 21 86072732.
E-mail address: hshokrollahi@khu.ac.ir; hassan_sh99@yahoo.com

Cracked nanorods have gained significant attention in the field of nanotechnology due to their unique properties and potential applications. These nanorods, which are typically made of materials such as gold or silver, undergo controlled cracking to create gaps or breaks along their length. This deliberate manipulation of nanorod structures opens up a range of practical applications in various fields. The main practical applications of cracked nanorods include sensing and detection, catalysis, optics, electronics, and energy conversion [2, 3].

A literature survey on the investigation of the effects of the crack on the mechanical behaviors of nanoscale structures shows that this issue has been examined in various cases. Here, the related references are categorized according to the shape of the nano-structure, plate, beam, bar, and rod.

For plate-like nanostructures, Wang et al. [4] have simulated micro-crack healing in copper nano-plate during heating using the molecular dynamics method. In another study, the crack propagation process in a single-crystal aluminum plate with central cracks under tensile load has been simulated by the molecular dynamics method [5]. Hu et al. [6] have studied the surface energy effect on the fracture behavior of thin films with Mode-I and mode-II cracks.

For beam-like structures, there are considerable studies. The studies have considered the effect of the crack on the mechanical behavior of beam-like nanostructures based on various theories. Based on the nonlocal elasticity theory, free transverse vibration of Euler-Bernoulli [7-10] and Timoshenko [11-14] nanobeams, functionally graded nanobeams [15, 16], nanobeams with multiple cracks [17], and nanobeams embedded in the elastic medium [12, 15, 18] have been studied. In addition, Khorshidi et al. [19] have investigated buckling and postbuckling behaviors of cracked nanobeams made of single-crystalline nano-materials incorporating the beam's axial stretching via von Karman nonlinear theory. There are also some studies based on the surface elasticity theory. In this regard, free transverse vibration of thin and thick nanobeams with single and mixed-mode cracks are investigated by considering the surface energy effects [12, 20-23]. The other studies on the mechanical behaviors of nano-beams are based on the modified couple stress theory. Bending [24], buckling and postbuckling [25, 26], and free transverse vibration [27-29] of cracked nanobeams have been analyzed based on the modified couple stress theory.

For bar-like nanostructures in which the torsional behavior is desired, Loya et al. [30] and Rahmani et al. [31] have considered the effect of the crack on free torsional vibration of nanobeams using the nonlocal elasticity theory. In addition, free torsional vibration of cracked nanobeams incorporating the surface energy effect has been investigated by Nazemnezhad and Fahimi [32].

Finally, there are a few studies in which the axial or longitudinal behaviors of nanostructures in the presence of the crack are analyzed. In references [33, 34] free axial vibration of cracked nanorods has been investigated based on the nonlocal elasticity theory. Furthermore, the elastic medium effect as well as the crack effect on the axial vibration of nanorods is studied based on the nonlocal elasticity theory [35].

The above literature survey shows that the works considered the effect of the crack on mechanical behaviors of nano-scale structures have implemented the nonlocal elasticity theory, the modified couple stress theory, and the surface elasticity theory. Among the four types of mentioned nanostructures, three of them, plate-like, beam-like, and bar-like nanostructures, have been analyzed using the surface elasticity theory. Since the theories give different results for a specific problem, it is necessary to have a comprehensive insight into the various aspects of the problem for future research. The importance of the present study comes from two main aspects. The first aspect lies in the methodology employed to model cracks and mathematically illustrate their impact on dynamic systems. This encompasses both the formulation of equations of motion and the consideration of boundary conditions. It is widely acknowledged or predictable that cracks tend to decrease the natural frequencies of a system by inducing structural softening. However, the equations of motion have been derived in a manner that necessitates the development of a new solution method. This highlights the requirement for an alternative approach, which may not have been necessary or utilized in other similar problems. The second aspect pertains to the utilization of the theory of surface elasticity. The distinction between this particular theory and other proposed theories, such as non-local theory, lies in its omission of a tuning or matching parameter within the equations. In other proposed theories, a parameter is introduced to bring the theoretical results closer to the simulation or laboratory results by adjusting its value. Typically, this parameter's value is contingent upon various conditions, even within a specific problem. However, this is not the case with the theory of surface elasticity. Instead, it solely deals with a series of surface mechanical properties whose values are considered fixed for a specific material. Therefore, it is important to examine the behavior of the structure from the perspective of this theory. To this end, governing equation of motion and corresponding boundary conditions of cracked nanorods incorporating the surface energy effects are obtained using Hamilton's principle. Due to considering the surface energy effect the obtained governing equation of motion becomes non-homogeneous. To extract the natural frequencies of the nanorod, firstly the non-homogeneous governing equation is converted to a homogeneous one using an appropriate change of variable, and then for clamped-clamped and clamped-free boundary conditions, the governing equation is solved using an analytical

method. To conduct comprehensive research, the effects of various parameters such as the length and radius of the nanorod, the crack severity, the crack position, the type of boundary condition, and the values of surface and bulk material properties on the axial frequencies of nanorod are investigated.

2 PROBLEM FORMULATION

Consider a thin nanorod having length L ($0 \le x \le L$) and cross section of A, in a Cartesian coordinate system xyz, as shown in Fig. 1.

According to the simple rod theory, the components of displacement (u, v, and w) are as follows [36]

$$u(x,y,z,t) = u(x,t) \tag{1}$$

$$v(x,y,z,t) = 0 \tag{2}$$

$$w(x,y,z,t) = 0 \tag{3}$$

in which t is the time in sec. Having these displacements, assuming the rod is made from an isotropic material, the strains and stresses can be defined as

$$\varepsilon_{xx} = \frac{\partial u}{\partial x} \tag{4}$$

$$\varepsilon_{yy} = \varepsilon_{zz} = \varepsilon_{xy} = \varepsilon_{xz} = \varepsilon_{yz} = 0 \tag{5}$$

$$\sigma_{xx} = E\frac{\partial u}{\partial x} \tag{6}$$

$$\sigma_{yy} = \sigma_{zz} = \sigma_{xy} = \sigma_{xz} = \sigma_{yz} = 0 \tag{7}$$

The Eqs. (4)-(7) are represented the strains and stresses related to the bulk material of the nanorod. If the surface energy effect is included in the analysis, the surface stress and strain components must be obtained. To this aim, the surface elasticity theory is proposed. In surface elasticity theory proposed by Gurtin and Murdoch [37], the relation between surface stress and strain can be expressed as

$$\tau_{\alpha\beta}^{\pm} = \tau_s^{\pm}\delta_{\alpha\beta} + \left(\mu_s^{\pm} - \tau_s^{\pm}\right)\left(u_{\alpha,\beta}^{\pm} + u_{\beta,\alpha}^{\pm}\right) + \left(\lambda_s^{\pm} + \tau_s^{\pm}\right)u_{m,m}\delta_{\alpha\beta} + \tau_s^{\pm}u_{\alpha,\beta} \tag{8}$$

$$\tau_{\alpha z}^{\pm} = \tau_s^{\pm}u_{z,\alpha} \tag{9}$$

in which $\tau_s^{\pm}$ is residual surface stress related to no strain condition, $\delta_{\alpha\beta}$ is Kronecker delta, $\lambda_s^{\pm}$ and $\mu_s^{\pm}$ are Lamé constants, $u_{\alpha,\beta}$ are surface displacement components, and $\alpha,\beta = x,y$. Note that the positive and the negative signs are represented for upper and lower surfaces of the nanorod (for rectangular or quadrangular cross sections). Since the nanorod in this study has circular cross section, the positive and negative signs are disregarded.

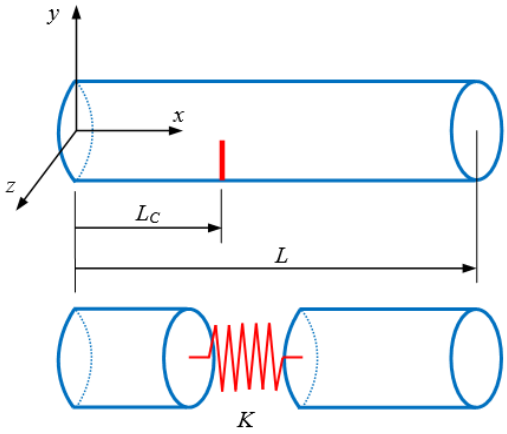

Fig.1
Schematic of a cracked nanorod and modeled configuration.

Using Eqs. (1)-(3), surface stresses effective to longitudinal vibration of nanorod are obtained as

$$\tau_{xx} = \tau_s + (\lambda_s + 2\mu_s)\frac{\partial u}{\partial x} \tag{10}$$

$$\tau_{yy} = \tau_{zz} = \tau_{xy} = \tau_{xz} = \tau_{yz} = 0 \tag{11}$$

In order to arrive to the governing equation and the boundary conditions, the bulk and surface stresses and strains must be used in Hamilton's principle defined by Eq. (12),

$$\int_{t_1}^{t_2} (\delta T - \delta U)dt = 0 \tag{12}$$

The variation of kinetic energy of nanorod take into account the effect of kinetic energy of surface density, can be written as

$$\delta T = \delta T^b + \delta T^s = \int_0^L \rho\left(\frac{\partial u(x,t)}{\partial t}\right)\delta\left(\frac{\partial u(x,t)}{\partial t}\right)A\,dx + \int_0^L \rho_s\left(\frac{\partial u(x,t)}{\partial t}\right)\delta\left(\frac{\partial u(x,t)}{\partial t}\right)S dx \tag{13}$$

in which ρ and ρ_s are bulk and surface density, respectively, and A and S are surface and periphery of nanorod, respectively. Substituting Eqs. (4) and (6) in forming the potential energy relation, the variation of potential energy can be expressed as

$$\delta U = \delta U^b + \delta U^s = \int_0^L E\frac{\partial u}{\partial x}\delta\left(\frac{\partial u}{\partial x}\right)A\,dx + \int_0^L \left(\tau_s + (\lambda_s + 2\mu_s)\frac{\partial u}{\partial x}\right)\delta\left(\frac{\partial u}{\partial x}\right)S dx \tag{14}$$

Substituting Eqs. (13) and (14) into Eq. (12), and integrating the resulted equation by part, the governing equation and the corresponding boundary conditions of cracked nanorods incorporating the surface energy effects are obtained as follows,

$$-(\rho A + \rho_s S)\frac{\partial^2 u(x,t)}{\partial t^2} + (EA + (\lambda_s + 2\mu_s)S)\frac{\partial^2 u(x,t)}{\partial x^2} = 0 \tag{15}$$

$$\left(S\tau_s + (EA + (\lambda_s + 2\mu_s)S)\frac{\partial u(x,t)}{\partial x}\right)\delta u\Big|_0^L = 0 \tag{16}$$

Assume that in the crack location ($x = L_C$) an equivalent linear spring K connecting the two segments of the nanorod, then for each segments of the nanorod, i.e. $0 \le x < L_C$ and $L_C < x \le L$, the Eqs. (15) and (16) must be applied. Implementing Eq. (15) leads to following equations,

$$-(\rho A)_{eq}\frac{\partial^2 u_1(x,t)}{\partial t^2} + (EA)_{eq}\frac{\partial^2 u_1(x,t)}{\partial x^2} = 0; \quad 0 \le x < L_C \tag{17}$$

$$-(\rho A)_{eq}\frac{\partial^2 u_2(x,t)}{\partial t^2} + (EA)_{eq}\frac{\partial^2 u_2(x,t)}{\partial x^2} = 0; \quad L_C < x \le L \tag{18}$$

where $(\rho A)_{eq} = \rho A + \rho_s S$ and $(EA)_{eq} = EA + (\lambda_s + 2\mu_s)S$.

In crack location, $x = L_C$, following continuity conditions must be satisfied,

$$K\left(u_1(L_C,t) - u_2(L_C,t)\right) = -\tau_s S - (EA)_{eq}\frac{\partial u_1(L_C,t)}{\partial x} \tag{19}$$

$$\frac{\partial u_1(L_C,t)}{\partial x} = \frac{\partial u_2(L_C,t)}{\partial x} \tag{20}$$

Moreover, end conditions of nanorod for clamped-clamped and clamped-free nanorods are as Eq. (21) and (22) respectively,

$$\begin{aligned} &u_1(0,t) = 0 \\ &u_2(L,t) = 0 \end{aligned} \tag{21}$$

$$\begin{aligned} &u_1(0,t) = 0 \\ &\frac{\partial u_2(L,t)}{\partial x} = -\frac{\tau_s S}{(EA)_{eq}} \end{aligned} \tag{22}$$

Eqs. (19) and (22) imply that the relation of boundary condition at the free end of the nanorod as well as one of the relations of the continuity conditions are inhomogeneous. Therefore, in order to solve the governing equations of motion, these relations must be homogenized at first.

It is worth mentioning here that it has not been reported in literature that homogeneous relations of boundary conditions and/or equations of motion are changed to inhomogeneous ones by considering the surface energy effects on various mechanical behaviors of nanosized structures. Therefore, the present study reports this issue for the first time.

In order to study the vibration characteristics of the cracked nanorod, Eqs. (17)-(20) along with Eq. (21) and (22) must be solved for the clamped-clamped and the clamped-free conditions, respectively. The method of solution of obtained equations is presented in next two subsections.

2.1 Clamped-clamped cracked nanorod

As mentioned before, the first step in solving the governing equations of motion is homogenization of Eqs. (19) and (22). At first, the equations and boundary conditions must be homogenized. To this aim it is supposed that

$$u_1(x,t) = v_{1cc}(x,t) + u_{1cc}(x) \tag{23}$$

$$u_2(x,t) = v_{2cc}(x,t) + u_{2cc}(x) \tag{24}$$

Substituting $u_1(x,t)$ and $u_2(x,t)$ into Eqs. (17)-(21), the related equations for $u_{1cc}(x)$ and $u_{2cc}(x)$ are obtained as follows

$$(EA)_{eq}\frac{d^2u_{1cc}(x)}{dx^2} = 0; \quad 0 \le x < L_C \tag{25}$$

$$(EA)_{eq}\frac{d^2u_{2cc}(x)}{dx^2} = 0; \quad L_C < x \le L \tag{26}$$

$$K\left(u_{1cc}(L_C) - u_{2cc}(L_C)\right) = -\tau_s S - (EA)_{eq}\frac{du_{1cc}(L_C)}{dx} \tag{27}$$

$$\frac{du_{1cc}(L_C)}{dx} = \frac{du_{2cc}(L_C)}{dx} \tag{28}$$

$$\begin{aligned} u_{1cc}(0) &= 0 \\ u_{2cc}(L) &= 0 \end{aligned} \tag{29}$$

Solving Eqs. (25)-(29) leads to

$$u_{1cc}(x) = \frac{-\tau_s S}{(EA)_{eq} + KL}x; \quad 0 \le x < L_C \tag{30}$$

$$u_{2cc}(x) = \frac{-\tau_s S}{(EA)_{eq} + KL}(x - L); \quad L_C < x \le L \tag{31}$$

Now, substituting Eqs. (30) and (31) into Eqs. (23) and (24) and using $u_1(x,t)$ and $u_2(x,t)$ in Eqs. (17)-(21) leads to following equations,

$$-(\rho A)_{eq}\frac{\partial^2 v_{1cc}(x,t)}{\partial t^2} + (EA)_{eq}\frac{\partial^2 v_{1cc}(x,t)}{\partial x^2} = 0; \quad 0 \le x < L_C \tag{32}$$

$$-(\rho A)_{eq}\frac{\partial^2 v_{2cc}(x,t)}{\partial t^2} + (EA)_{eq}\frac{\partial^2 v_{2cc}(x,t)}{\partial x^2} = 0; \quad L_C < x \le L \tag{33}$$

$$EA\left(v_{1cc}(L_C,t) - v_{2cc}(L_C,t)\right) = -CL(EA)_{eq}\frac{\partial v_{1cc}(L_C,t)}{\partial x} \tag{34}$$

$$\frac{\partial v_{1cc}(L_C,t)}{\partial x} = \frac{\partial v_{2cc}(L_C,t)}{\partial x} \tag{35}$$

$$v_{1cc}(0,t)=0$$
$$v_{2cc}(L,t)=0 \tag{36}$$

where $C=\dfrac{EA}{KL}$. Assuming harmonic displacements as

$$v_{1cc}(x,t)=V_{1cc}(x)T(t)=V_{1cc}(x)e^{i\omega t} \tag{37}$$

$$v_{2cc}(x,t)=V_{2cc}(x)T(t)=V_{2cc}(x)e^{i\omega t} \tag{38}$$

Eqs. (32)-(36) can be rewritten as

$$\omega^2(\rho A)_{eq}V_{1cc}(x)+(EA)_{eq}\frac{d^2V_{1cc}(x)}{dx^2}=0;\quad 0\le x<L_C \tag{39}$$

$$\omega^2(\rho A)_{eq}V_{2cc}(x)+(EA)_{eq}\frac{d^2V_{2cc}(x)}{dx^2}=0;\quad L_C<x\le L \tag{40}$$

$$EA\left(V_{1cc}(L_C)-V_{2cc}(L_C)\right)=-CL(EA)_{eq}\frac{dV_{1cc}(L_C)}{dx} \tag{41}$$

$$\frac{dV_{1cc}(L_C)}{dx}=\frac{dV_{2cc}(L_C)}{dx} \tag{42}$$

$$V_{1cc}(0)=0$$
$$V_{2cc}(L)=0 \tag{43}$$

The solutions of Eqs. (39) and (40) are

$$V_{1cc}(x)=A_1\sin\frac{\omega x}{c}+B_1\cos\frac{\omega x}{c} \tag{44}$$

$$V_{2cc}(x)=A_2\sin\frac{\omega x}{c}+B_2\cos\frac{\omega x}{c} \tag{45}$$

where $c^2=\dfrac{(EA)_{eq}}{(\rho A)_{eq}}$.

Application of Eqs. (41)-(43) leads to $B_1 = 0$ and following system of equations,

$$\begin{bmatrix} 0 & \sin\dfrac{\omega L}{c} & \cos\dfrac{\omega L}{c} \\ -\cos\dfrac{\omega L_C}{c} & \cos\dfrac{\omega L_C}{c} & -\sin\dfrac{\omega L_C}{c} \\ \sin\dfrac{\omega L_C}{c}+\dfrac{\omega}{c}\dfrac{CL(EA)_{eq}}{EA}\cos\dfrac{\omega L_C}{c} & -\sin\dfrac{\omega L_C}{c} & -\cos\dfrac{\omega L_C}{c} \end{bmatrix}\begin{Bmatrix} A_1 \\ A_2 \\ B_2 \end{Bmatrix}=0 \tag{46}$$

To have a nontrivial solution, determinant of coefficient matrix must set to be zero. The resulted equation is as follows

$$\cos\frac{\omega(2L_C-L)}{c}+\cos\frac{\omega L}{c}+\frac{2cEA}{\omega CL(EA)_{eq}}\sin\frac{\omega L}{c}=0 \tag{47}$$

Solving Eq. (47) numerically, using MATLAB software, the natural frequencies of the clamped-clamped cracked nanorod are obtained.

2.2 Clamped-free cracked nanorod

Similar to section 2.1, suppose that $u_1(x,t)=v_{1cf}(x,t)+u_{1cf}(x)$ and $u_2(x,t)=v_{2cf}(x,t)+u_{2cf}(x)$. Substituting $u_1(x,t)$ and $u_2(x,t)$ into Eqs. (17)-(20) and (22), the related equations for $u_{1cf}(x)$ and $u_{2cf}(x)$ are obtained as follows

$$(EA)_{eq}\frac{d^2u_{1cf}(x)}{dx^2}=0;\quad 0\le x<L_C \tag{48}$$

$$(EA)_{eq}\frac{d^2u_{2cf}(x)}{dx^2}=0;\quad L_C<x\le L \tag{49}$$

$$K\left(u_{1cf}(L_C)-u_{2cf}(L_C)\right)=-\tau_s S-(EA)_{eq}\frac{du_{1cf}(L_C)}{dx} \tag{50}$$

$$\frac{du_{1cf}(L_C)}{dx}=\frac{du_{2cf}(L_C)}{dx} \tag{51}$$

$$u_{1cf}(0)=0$$

$$\frac{du_{2cf}(L)}{dx}=-\frac{\tau_s S}{(EA)_{eq}} \tag{52}$$

Solving Eqs. (48)-(52) leads to,

$$u_{1cf}(x)=\frac{-\tau_s S}{(EA)_{eq}}x;\quad 0\le x<L_C \tag{53}$$

$$u_{2cf}(x)=\frac{-\tau_s S}{(EA)_{eq}}x;\quad L_C<x\le L \tag{54}$$

Now, substituting Eqs. (53) and (54) into $u_1(x,t)=v_{1cf}(x,t)+u_{1cf}(x)$ and $u_2(x,t)=v_{2cf}(x,t)+u_{2cf}(x)$ and using $u_1(x,t)$ and $u_2(x,t)$ in Eqs. (17)-(20) and (22) leads to following equations,

$$-(\rho A)_{eq}\frac{\partial^2 v_{1cf}(x,t)}{\partial t^2}+(EA)_{eq}\frac{\partial^2 v_{1cf}(x,t)}{\partial x^2}=0;\quad 0\le x<L_C \tag{55}$$

$$-(\rho A)_{eq}\frac{\partial^2 v_{2cf}(x,t)}{\partial t^2}+(EA)_{eq}\frac{\partial^2 v_{2cf}(x,t)}{\partial x^2}=0;\quad L_C<x\le L \tag{56}$$

$$EA\left(v_{1cf}(L_C,t)-v_{2cf}(L_C,t)\right)=-CL(EA)_{eq}\frac{\partial v_{1cf}(L_C,t)}{\partial x} \tag{57}$$

$$\frac{\partial v_{1cf}(L_C,t)}{\partial x}=\frac{\partial v_{2cf}(L_C,t)}{\partial x} \tag{58}$$

$$v_{1cf}(0,t)=0$$

$$\frac{\partial v_{2cf}(L,t)}{\partial x}=0 \tag{59}$$

Assuming harmonic displacements as $v_{1cf}(x,t)=V_{1cf}(x)T(t)=V_{1cf}(x)e^{i\omega t}$ and $v_{2cf}(x,t)=V_{2cf}(x)T(t)=V_{2cf}(x)e^{i\omega t}$, Eqs. (55)-(59) can be rewritten as

$$\omega^2(\rho A)_{eq}V_{1cf}(x)+(EA)_{eq}\frac{d^2V_{1cf}(x)}{dx^2}=0;\quad 0\le x<L_C \tag{60}$$

$$\omega^2(\rho A)_{eq}V_{2cf}(x)+(EA)_{eq}\frac{d^2V_{2cf}(x)}{dx^2}=0;\quad L_C<x\le L \tag{61}$$

$$EA\left(V_{1cf}(L_C)-V_{2cf}(L_C)\right)=-CL(EA)_{eq}\frac{dV_{1cf}(L_C)}{dx} \tag{62}$$

$$\frac{dV_{1cf}(L_C)}{dx}=\frac{dV_{2cf}(L_C)}{dx} \tag{63}$$

$$V_{1cf}(0)=0$$

$$\frac{dV_{2cf}(L)}{dx}=0 \tag{64}$$

The solution of Eqs. (60) and (61) are $V_{1cf}(x) = A_1 \sin\frac{\omega x}{c} + B_1 \cos\frac{\omega x}{c}$ and $V_{2cf}(x) = A_2 \sin\frac{\omega x}{c} + B_2 \cos\frac{\omega x}{c}$ where $c^2 = \frac{(EA)_{eq}}{(\rho A)_{eq}}$. Application of Eqs. (62)-(64) leads to $B_1 = 0$ and following system of equations,

$$\begin{bmatrix} 0 & \cos\frac{\omega L}{c} & -\sin\frac{\omega L}{c} \\ -\cos\frac{\omega L_C}{c} & \cos\frac{\omega L_C}{c} & -\sin\frac{\omega L_C}{c} \\ \sin\frac{\omega L_C}{c} + \frac{\omega}{c}\frac{CL(EA)_{eq}}{EA}\cos\frac{\omega L_C}{c} & -\sin\frac{\omega L_C}{c} & -\cos\frac{\omega L_C}{c} \end{bmatrix} \begin{Bmatrix} A_1 \\ A_2 \\ B_2 \end{Bmatrix} = 0 \tag{65}$$

To have a nontrivial solution, determinant of coefficient matrix must set to be zero. The resulted equation is as following,

$$\sin\frac{\omega(2L_C - L)}{c} - \sin\frac{\omega L}{c} + \frac{2cEA}{\omega CL(EA)_{eq}}\cos\frac{\omega L}{c} = 0 \tag{66}$$

Solving Eq. (66) numerically, using MATLAB software, the natural frequencies of the clamped-free cracked nanorod are obtained.

3 RESULTS AND DISCUSSIONS

To verify the applicability and accuracy of the present formulation, two comparison studies are conducted. At first, the results of the present study are compared with those reported by Rao [36] and Nazemnezhad and Shokrollahi [38] for an intact nanorod, without considering the surface energy effects. Ref. [36] provided the longitudinal vibration of nanorods based on classical theory to study the behavior of macro-scale rods and in Ref. [38] the longitudinal vibration of nanorods using surface elasticity theory is presented. For evaluation of the first five natural longitudinal frequencies, this comparative study between the present solution without considering surface energy effects and the crack ($C = 0$) and the results given by Rao [36] and Nazemnezhad and Shokrollahi [38] is carried out in Table 1 for a rod with fixed-fixed and fixed-free boundary conditions, and $L = 10$ nm, $R = 1$ nm, $E = 70$ GPa, and $\rho = 2\ 700$ kg/m^3. As shown in Table 1, the reliability of the present formulation and results is confirmed. In the second comparison study, the results of the present analysis are compared with those reported by Nazemnezhad and Shokrollahi [39] using the numerical method (differential quadrature method). The results for a rod with fixed-fixed and fixed-free boundary conditions, with two different crack severities, C, and $L = 30$ nm, $R = 0.5$ nm, $E = 70$ GPa, $\rho = 2\ 700$ kg/m^3, $\mu_s = -0.8269$ N/m, $\lambda_s = 6.842$ N/m, $\rho_s =$k 5.46×10^{-7} kg/m^3, and $\tau_s = 0.5689$ N/m, are presented in Table 2. Again, the reliability of the present formulation and results is confirmed. As presented in Table 2, for lower frequencies there are the same results obtained using two methods, but by increasing the mode number the difference between results is evidenced.

Table 1
Comparison of natural frequencies of an intact nanorod (GHz).

Mode	Fixed-Fixed			Fixed-Free		
	Present	Ref. [38]	Ref. [36]	Present	Ref. [38]	Ref. [36]
1	254.59	254.59	254.59	127.29	127.29	127.29
2	509.18	509.18	509.18	381.88	381.88	381.88
3	763.76	763.76	763.76	636.47	636.47	636.47
4	1018.35	1018.35	1018.35	891.06	891.06	891.06
5	1272.94	1272.94	1272.94	1145.64	1145.64	1145.64

Table 2
Comparison of natural frequencies of a cracked nanorod (GHz).

Mode	C	Fixed-Fixed		Fixed-Free	
		Present	Ref. [39]	Present	Ref. [39]
1	0	71.8441	71.8441	35.9220	35.9250
	1	71.8441	71.8441	22.8006	22.8006
2	0	143.6881	143.6881	107.7661	107.7661
	1	89.0891	89.0891	81.2154	81.2154
3	0	215.5322	215.5323	179.6102	179.6103
	1	215.5322	215.5260	149.0046	149.0039
4	0	287.3763	287.3445	251.4543	251.4635
	1	222.7173	222.7094	219.1817	219.1746

Next, the effects of some parameters on the natural frequency of cracked nanorods are investigated. In all following case studies, the mechanical surface and bulk properties are considered as presented in Table 3.

Table 3
Material properties of cracked nanorod.

Material property	E (GPa)	μ_s (N/m)	λ_s (N/m)	ρ (kg/m^3)	ρ_s (kg/m^3)	τ_s (N/m)
Aluminum	70	-0.8269	6.8420	2700	5.46×10^{-7}	0.5689
Silicon	210	-2.7779	-5.0985	2370	3.17×10^{-7}	0.6056

It should be noted that the following abbreviations are used in the figures and tables:

$$\text{FR} = \frac{\text{classical frequency}}{\text{classical frequency}}$$

$$\text{FR-}\mu s\&\lambda s = \frac{\text{Frequency with surface Lamé, no crack}}{\text{classical frequency}}$$

$$\text{FR-}\rho s = \frac{\text{Frequency with surface density, no crack}}{\text{classical frequency}}$$

$$\text{FR-}\mu s\&\lambda s\text{-}\rho s = \frac{\text{Frequency with surface Lamé and surface density, no crack}}{\text{classical frequency}}$$

$$\text{FR-C} = \frac{\text{Frequency without surface effect, having crack}}{\text{classical frequency}}$$

$$\text{FR-C-}\mu s\&\lambda s = \frac{\text{Frequency with surface Lamé, having crack}}{\text{classical frequency}}$$

$$\text{FR-C-}\rho s = \frac{\text{Frequency with surface density, having crack}}{\text{classical frequency}}$$

$$\text{FR-C-}\mu s\&\lambda s\text{-}\rho s = \frac{\text{Frequency with surface Lamé and surface density, having crack}}{\text{classical frequency}}$$

FR: Frequency ratio without surface effect, no crack
FR-μs&λs: Frequency ratio with surface Lamé, no crack
FR-ρs: Frequency ratio with surface density, no crack
FR-μs&λs-ρs: Frequency ratio with surface Lamé and surface density, no crack
FR-C: Frequency ratio without surface effect, having crack
FR-C-μs&λs: Frequency ratio with surface Lamé, having crack
FR-C-ρs: Frequency ratio with surface density, having crack
FR-C-μs&λs-ρs: Frequency ratio with surface Lamé and surface density, having crack

where the classical frequency is the one obtained without considering effects of the surface parameters and the crack.

In order to study the effect of crack location on the natural frequency of nanorod, a cracked nanorod with fixed-fixed and fixed-free boundary conditions, and $L = 10$ nm, $R = 1$ nm, and $C = 2$ is considered.

The first three natural frequencies are depicted in Figs. 2 and 3 for fixed-fixed and fixed-free boundaries, respectively. Figs. 2 and 3 show that including the surface Lamé leads to increasing natural frequencies for the aluminum nanorod and decreasing natural frequencies for the silicon nanorod. This is explainable by referring to Table 3, where for aluminum the value of $\lambda_s + 2\mu_s$ is positive while for silicon is negative. Generally, the figures show that for aluminum nanorods the sequence of presence of the curves from higher frequencies to lower ones is as FR-μs&λs, FR, FR-μs&λs-ρs, FR-ρs, FR-C-μs&λs, FR-C, FR-C-μs&λs-ρs, FR-C-ρs. For silicon nanorods, this sequence is as FR, FR-μs&λs, FR-ρs, FR-μs&λs-ρs, FR-C, FR-C-μs&λs, FR-C-ρs, FR-C-μs&λs-ρs. Note that the abovementioned sequence is observed for all modes of longitudinal vibration, where the first three modes are presented in Figs. 2 and 3, and other modes are not reported here for the sake of brevity. It is observed that the FR-ρs is lower than FR, and FR-μs&λs-ρs is lower than FR-μs&λs for both aluminum and silicon nanorods. In other words, a decreasing effect of surface density on the frequency ratios of nanorods is seen. This is due to increasing the mass and the reverse effect of mass on natural frequencies. On the other hand, as noted above, including the surface Lamé leads to increasing natural frequencies for aluminum nanorods and decreasing natural frequencies for silicon nanorods. However, when the surface Lamé and surface density are included simultaneously, a decreasing effect on natural frequencies is observed for both materials. Besides, including cracks leads to a decrease in the natural frequencies. However, the sequence observed for cracked nanorods is the same as the one for nanorods without cracks, for both materials and two boundary conditions.

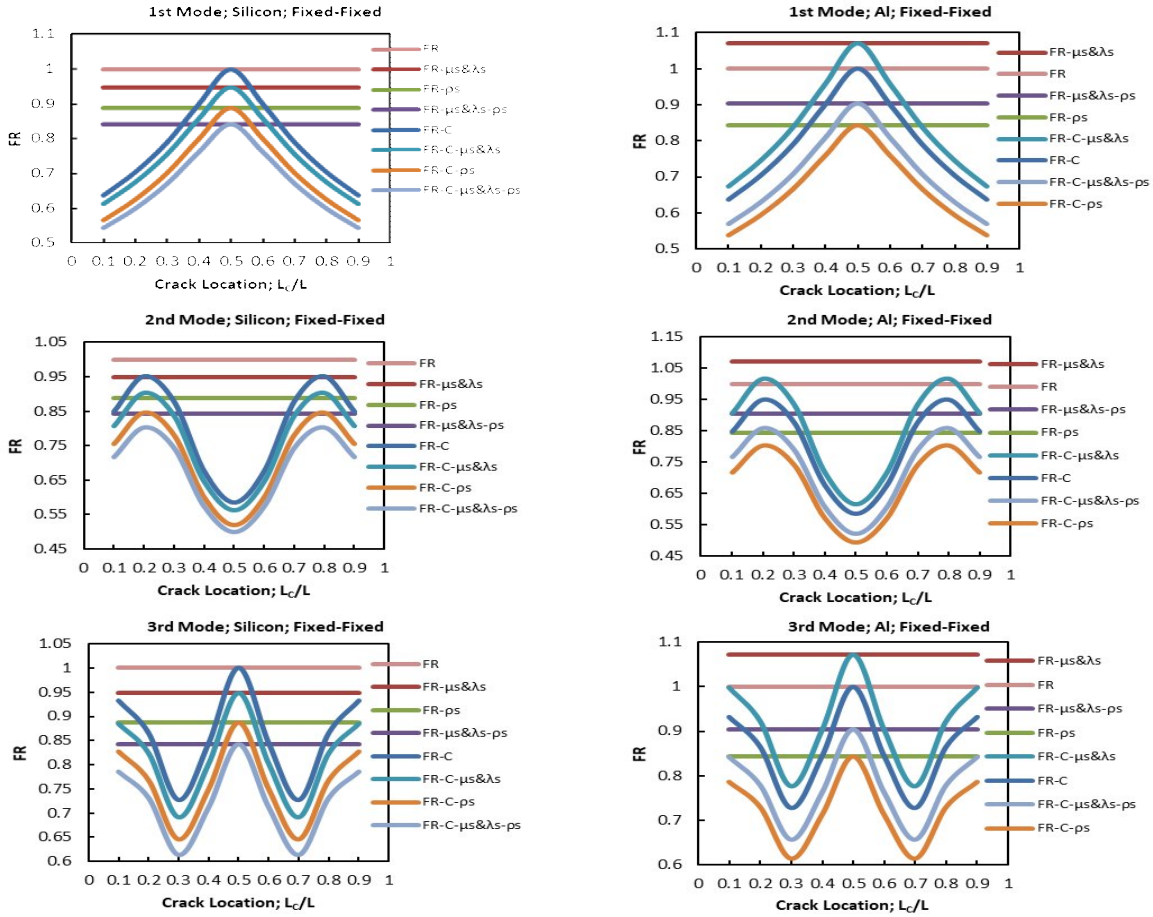

Fig.2
First three longitudinal frequency ratios of aluminum and silicon nanorods with fixed-fixed boundary conditions for different crack locations.

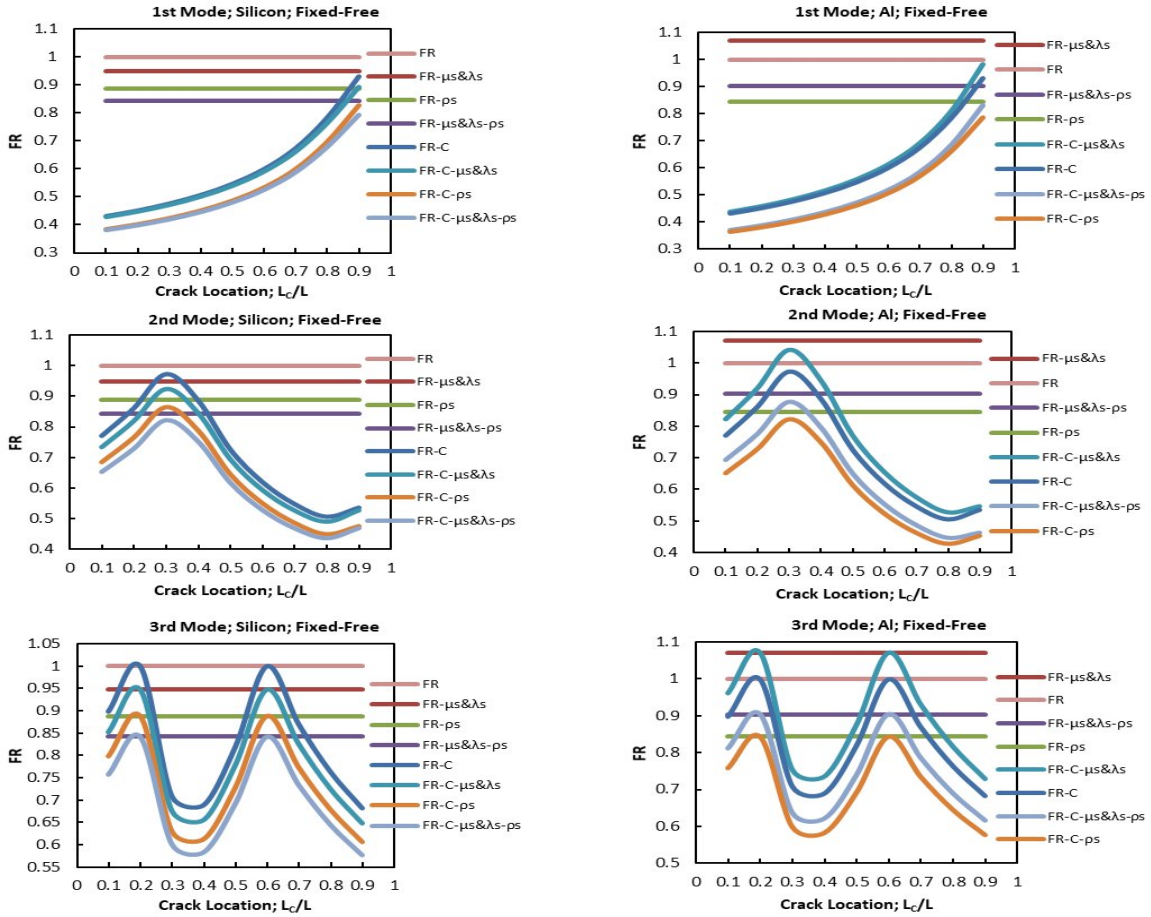

Fig.3
First three longitudinal frequency ratios of aluminum and silicon nanorods with fixed-free boundary conditions for different crack locations.

As shown in Figs. 2 and 3, the crack location has significant effects on the vibration behavior of nanorods. In Fig. 2 which is related to the fixed-fixed boundary condition, the symmetry is seen in results along crack location, which is because of the symmetry of the boundary condition. In this figure, the extremums are obtained for the frequencies by supposing the crack in the midsection of the nanorod in which these are maximum for the first and third modes and minimum for the second mode. However, for the second mode, there are maximums for crack locations of 0.2 and 0.8. Moreover, for the first and third modes, there are minimums at 0.3 and 0.7 crack locations.

On the other hand, Fig. 3 shows that as the crack is assumed to be near the fixed end, a larger decrease in the first natural frequency is observed than that closer to the free end. The reason is that as the crack location is closer to the fixed end the elastic strain energy of the cracked nanorod gradually decreases. However, for the second and third modes different trends are seen for changing crack location in nanorods. It is mainly because of the differences between these mode shapes for the fixed-free boundary condition. Moreover, the results show that for fixed-free nanorods the sequence of the presence of the frequency curves is the same as in fixed-fixed nanorods. It can be said that the effect of the surface energy is significant regardless of the type of boundary conditions.

To compare the effect of crack on the different modes of vibration, the frequency ratios for two different crack locations are listed in Table 4. The values in this table are presented for a better comparison of the effects of different parameters on the frequency ratios. As listed in Table 4, including crack leads to a decrease in the frequency ratios of nanorods. Note that the decreasing effect of the crack is due to the loss of rigidity of the structure; by decreasing the rigidity of the nanorod the frequency ratios decrease. As can be seen in Table 4, including the crack in nanorod, there are different modes (mode 1 or 2) that are affected more than others, for different crack locations. However, the frequency ratios for all modes are equal when there is no crack in the nanorod. Also, it is observed that in the absence of a crack, the effect of the surface energy is the same for different types of boundary conditions.

In another study, the effect of nanorod length is investigated. A cracked nanorod with fixed-fixed and fixed-free boundary conditions, R = 1 nm, C = 2, and $L_C = L/2$ are considered. The first and second natural frequencies are depicted in Figs. 4-7 for aluminum and silicon nanorods with different boundary conditions.

Table 4
First five longitudinal frequency ratios of aluminum and silicon nanorods with fixed-fixed and fixed-free boundary conditions for two different crack positions.

Frequency ratio	Frequency number	Fixed-Fixed				Fixed-Free			
		Aluminum		Silicon		Aluminum		Silicon	
		L_c/L=0.1	L_c/L=0.5	L_c/L=0.1	L_c/L=0.5	L_c/L=0.2	L_c/L=0.7	L_c/L=0.2	L_c/L=0.7
FR-C	Mode 1	0.638001	1.000000	0.638001	1.000000	0.452522	0.674934	0.452521	0.674934
	Mode 2	0.848998	0.584607	0.848998	0.584607	0.862112	0.547989	0.862112	0.547989
	Mode 3	0.932198	1.000000	0.932198	1.000000	1.000000	0.869945	1.000000	0.869945
	Mode 4	0.975460	0.766465	0.975460	0.766465	0.748553	0.965305	0.748553	0.965305
	Mode 5	1.000000	1.000000	1.000000	1.000000	0.837227	0.799069	0.837227	0.799069
FR-μs&λs-ρs	Mode 1	0.904197	0.904197	0.841958	0.841958	0.904197	0.904197	0.841958	0.841958
	Mode 2	0.904197	0.904197	0.841958	0.841958	0.904197	0.904197	0.841958	0.841958
	Mode 3	0.904197	0.904197	0.841958	0.841958	0.904197	0.904197	0.841958	0.841958
	Mode 4	0.904197	0.904197	0.841958	0.841958	0.904197	0.904197	0.841958	0.841958
	Mode 5	0.904197	0.904197	0.841958	0.841958	0.904197	0.904197	0.841958	0.841958
FR-C-μs&λs-ρs	Mode 1	0.568837	0.904197	0.543437	0.841958	0.386711	0.583477	0.397605	0.587209
	Mode 2	0.765952	0.52015	0.716188	0.498836	0.776612	0.48709	0.728142	0.468137
	Mode 3	0.842205	0.904197	0.785421	0.841958	0.904197	0.78518	0.841958	0.733599
	Mode 4	0.881665	0.69116	0.821568	0.646848	0.673039	0.871484	0.633299	0.813799
	Mode 5	0.904197	0.904197	0.841958	0.841958	0.756549	0.721786	0.705295	0.673399

As can be seen in Figs. 4-7, increasing the length of the nanorod leads to decreasing natural frequency. However, the frequency ratios are constant when the length of the nanorod increases. This is indicated that the amounts of changes in the nanorod frequencies caused by each surface energy parameter are the same for different lengths of nanorods. So, having the value of a frequency along with the frequency ratio for a distinct length of the nanorod, by using the frequency in other lengths, the frequency of the nanorod including any surface energy parameters can be determined. Again, the results show that the cracked nanorod is sensitive to surface energy parameters. For aluminum nanorods, including surface Lamé parameters leads the frequencies to increase. For other surface energy parameters, i.e. surface density and surface density together with surface Lamé leads the frequencies to decrease. This can be explained by considering that the surface Lamé affects the stiffness of the nanorod and surface density changes the nanorod mass. Any change in stiffness directly changes the natural frequencies. On the other hand, the mass has a reverse effect on the natural frequency of the nanorod. Moreover, except for 1st mode in Figs. 4 and 6 in which imposing a crack on the nanorod does not affect the frequency, the crack has a decreasing effect on the frequency and frequency ratio.

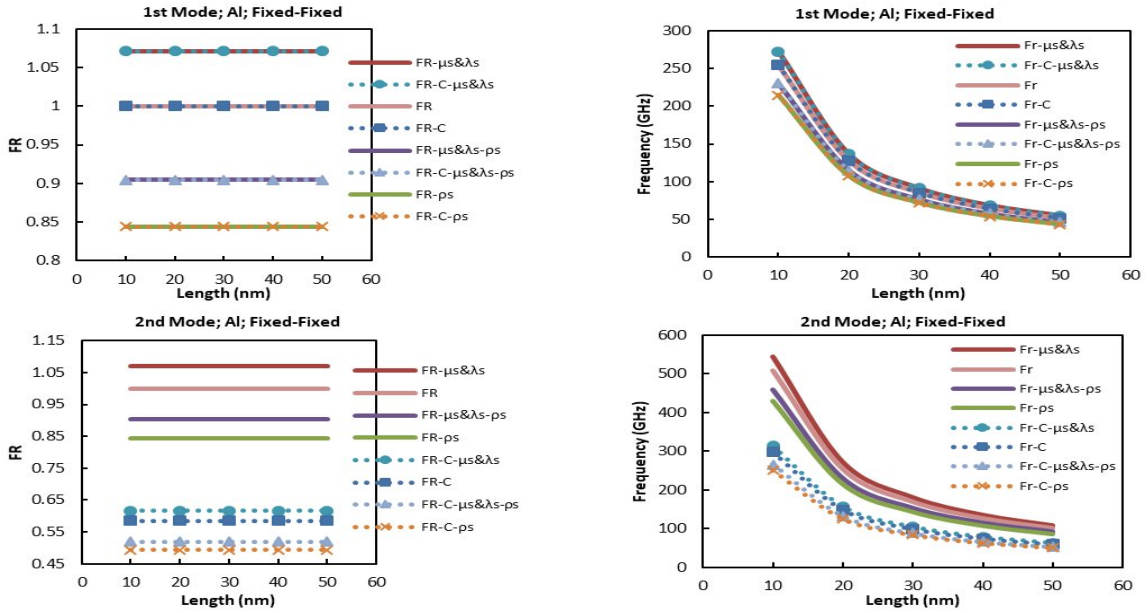

Fig.4
First and second longitudinal frequencies and frequency ratios of aluminum nanorods with fixed-fixed boundary conditions for different lengths.

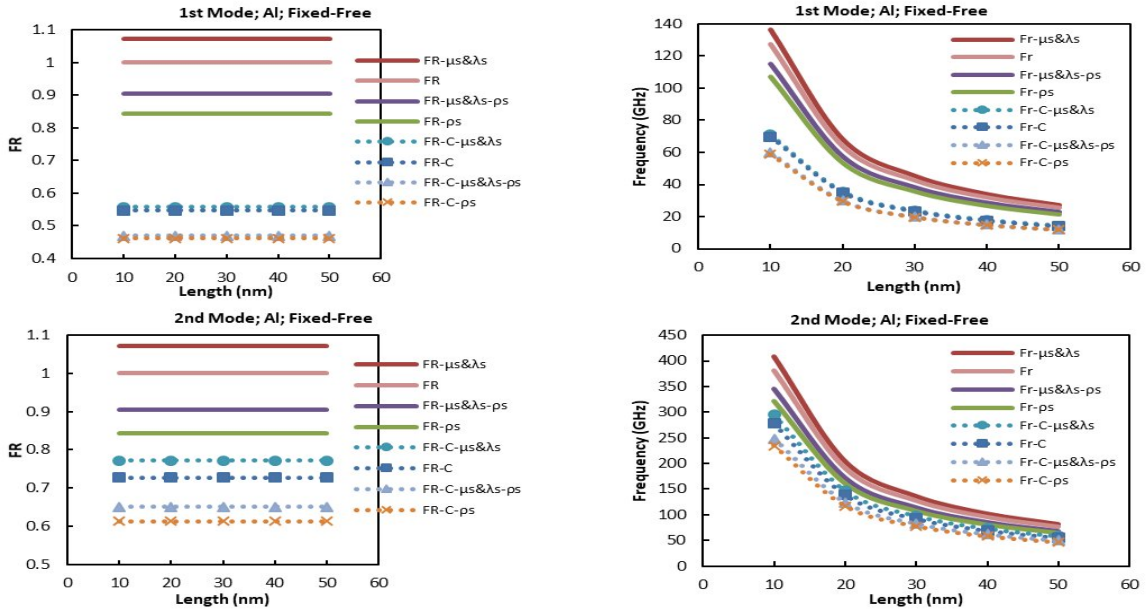

Fig.5
First and second longitudinal frequencies and frequency ratios of aluminum nanorods with fixed-free boundary conditions for different lengths.

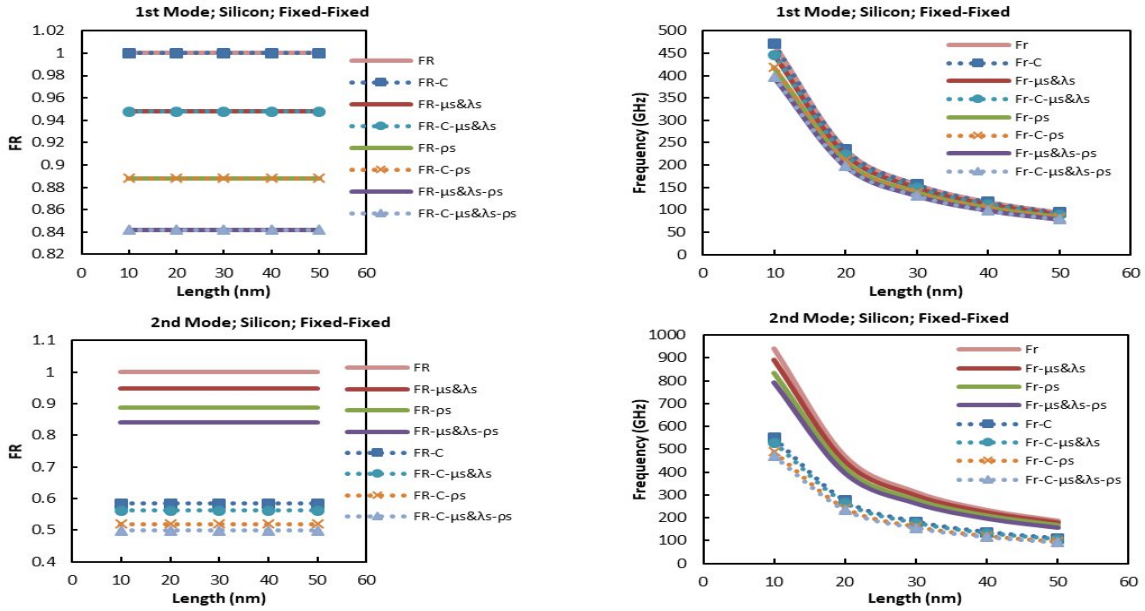

Fig.6
First and second longitudinal frequencies and frequency ratios of silicon nanorods with fixed-fixed boundary conditions for different lengths.

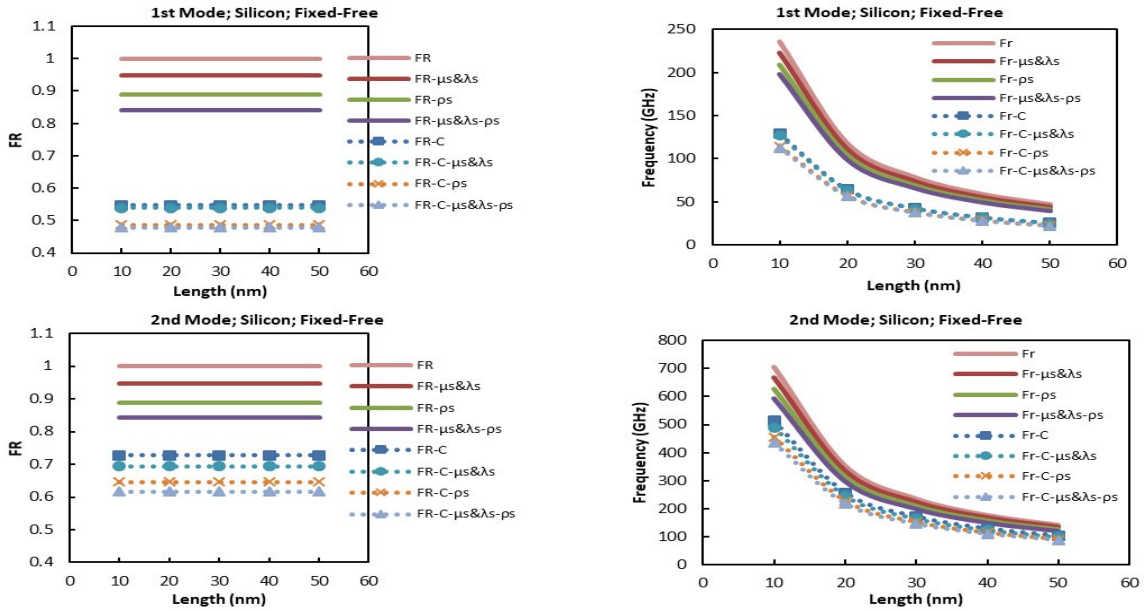

Fig.7
First and second longitudinal frequencies and frequency ratios of silicon nanorods with fixed-free boundary conditions for different lengths.

Another study has been done for different values of nanorod radius. A cracked nanorod with fixed-fixed and fixed-free boundary conditions, and L = 100 nm, C = 2, and $L_C = L/2$ are considered. The first and second natural frequencies are depicted in Figs. 8 and 9 for aluminum and silicon nanorods with fixed-fixed and fixed-free boundary conditions, respectively.

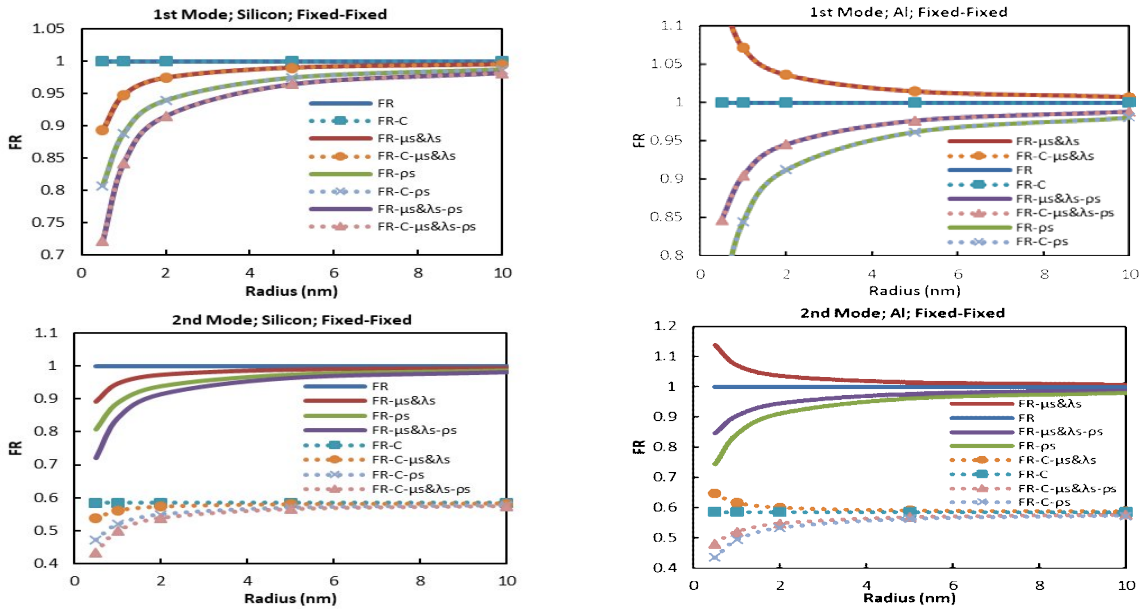

Fig.8
First and second longitudinal frequency ratios of aluminum and silicon nanorods with fixed-fixed boundary conditions for different radiuses.

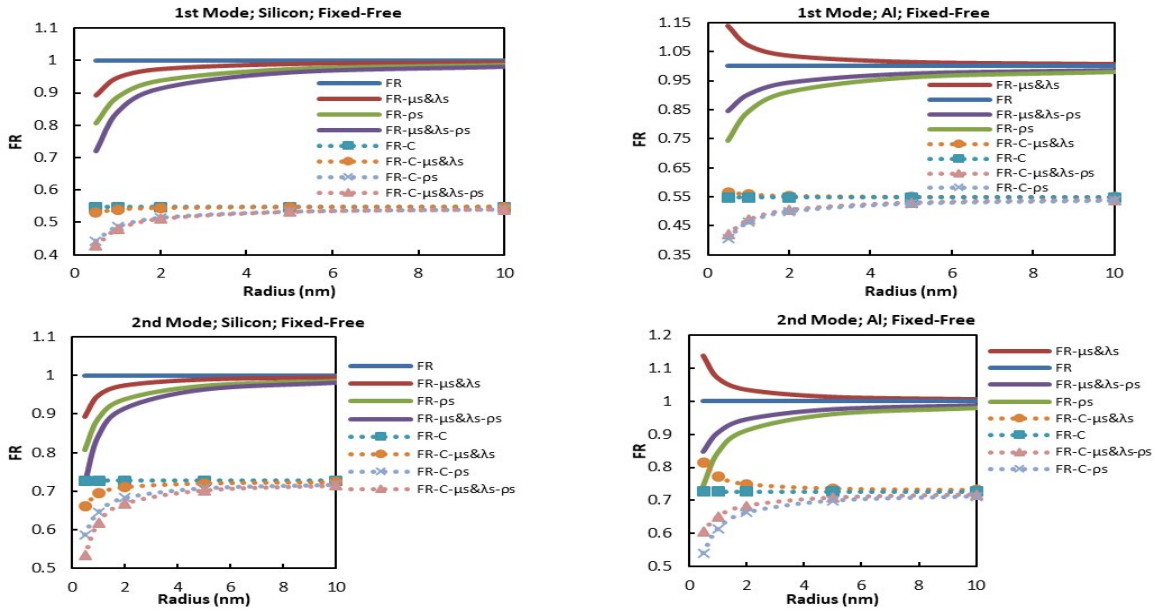

Fig.9
First and second longitudinal frequency ratios of aluminum and silicon nanorods with fixed-free boundary conditions for different radiuses.

As shown in Figs. 8 and 9, the cracked nanorod is sensitive to surface energy parameters. However, increasing the radius of the nanorod leads to decreasing the effect of surface energy on frequency ratios. As before, for aluminum nanorods, including surface Lamé parameters leads the frequency ratios to increase. Including other surface energy parameters, i.e. surface density and surface density together with surface Lamé, leads the frequency ratios to decrease. Again, the crack has a decreasing effect on the frequency ratio. Moreover, it can be seen that by

increasing the radius of the nanorod, the frequency ratio approaches the curve without including the surface effects. In other words, for nanorods with a large radius, the effect of the surface energy on frequency ratios is negligible.

The effects of crack severity parameter C, are investigated in a different study. To this end, variations of the first two longitudinal frequency ratios for cracked nanorods versus the crack severity parameter C are shown in Figs. 10 and 11 for different boundary conditions and $L = 10$ nm, $R = 1$ nm, and $L_C = L/2$.

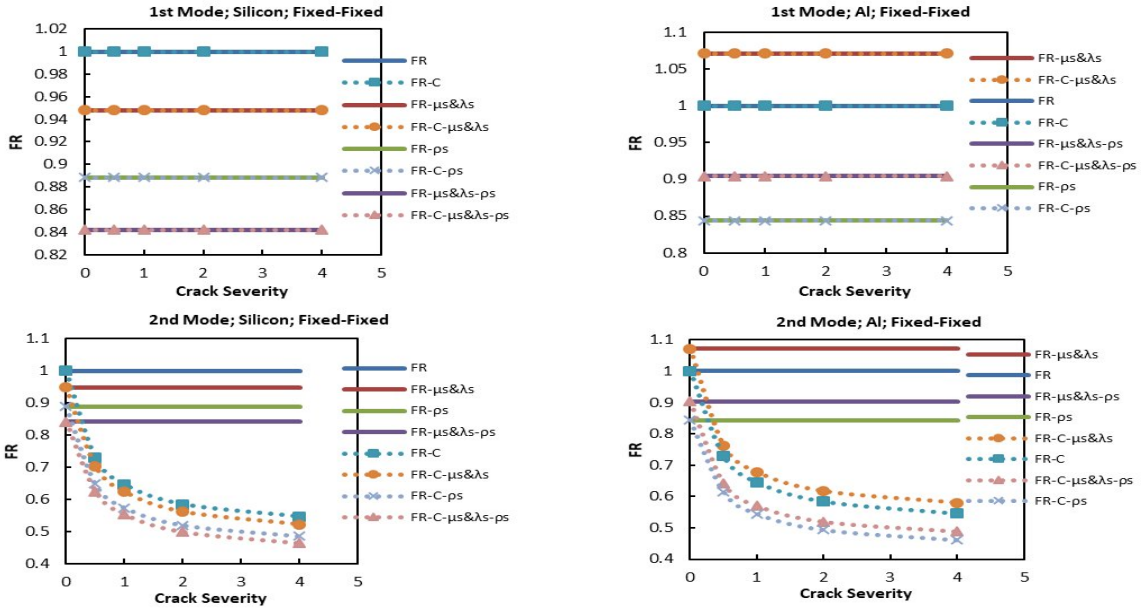

Fig.10
First and second longitudinal frequency ratios of aluminum and silicon nanorods with fixed-fixed boundary conditions for different crack severities.

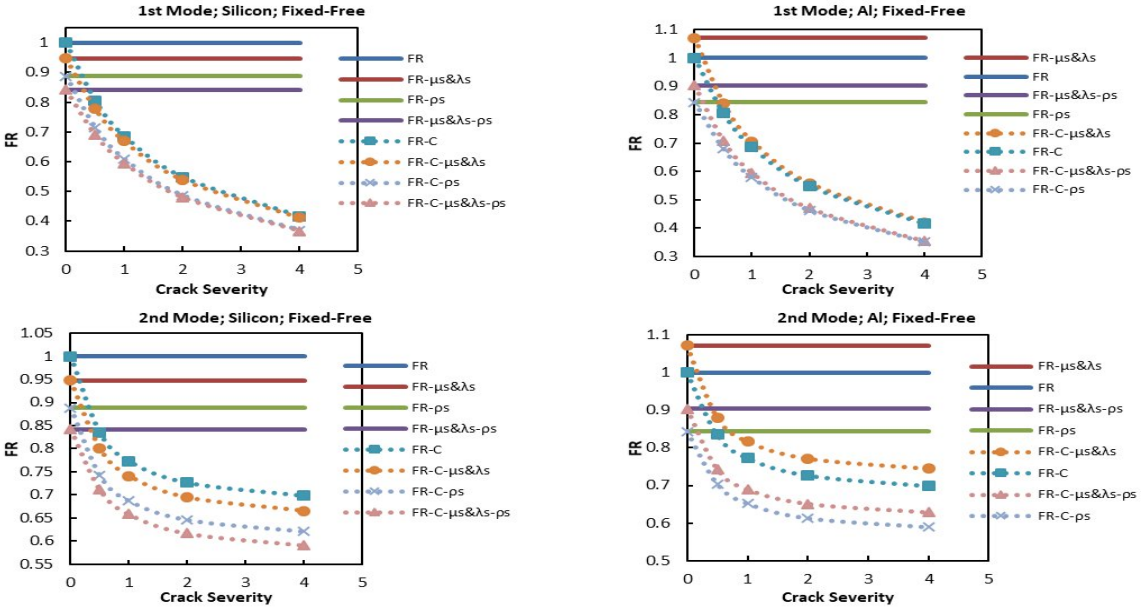

Fig.11
First and second longitudinal frequency ratios of aluminum and silicon nanorods with fixed-free boundary conditions for different crack severities.

Figures 10 and 11 illustrate that the effect of the surface energy on the longitudinal frequency ratios is independent of the crack severity, but the effect of the crack on longitudinal frequency ratios intensively depends on the crack severity. By increasing the crack severity, the frequency ratios are decreased. Besides, Figs. 10 and 11 show that for silicon nanorods both surface energy and crack have decreasing effects. Meanwhile for aluminum nanorods, including surface Lamé parameters leads the frequency ratios to increase but including crack leads the frequency ratios to decrease. So as can be seen in these figures, there is a crack severity value in which the increasing effect of surface energy and decreasing effect of crack, cancel out each other and consequently, the frequency remains unchanged. We name this value as special crack severity C^*. In the case of the mentioned cracked nanorod, the C^* is obtained for different crack locations and the result is depicted in Fig. 12 for the first two modes and different boundary conditions.

4 CONCLUSIONS

The free longitudinal vibration of nanorods in the presence of the crack is studied analytically based on the surface elasticity theory. Governing differential equation of motion and corresponding boundary conditions of cracked nanorods are obtained using Hamilton's principle. Due to considering the surface stress effect as well as the surface density and the surface Lamé constants the obtained governing equation of motion becomes non-homogeneous. The non-homogeneous governing equation is solved using appropriate analytical methods and natural frequencies are extracted. This research can pave the way for other researchers to better examine issues such as the effect of the type of material (functionally graded, etc.), the type of environment in which the structure is placed (elastic substrate or under the influence of temperature or magnetic environment), or even the type of problem (non-linearity). Based on this study, the following are concluded:

- In the presence of surface energy parameters, the crack location has significant effects on the vibration behavior of nanorods.
- The crack has a decreasing effect on the frequency ratios of nanorods.
- Including the crack in nanorod, the first or second mode of vibration is affected more than others, for different crack locations.
- Increasing the radius of nanorod leads to decreasing the effect of surface energy on frequency ratios.
- The effect of the surface energy on the longitudinal frequency ratios is independent of the crack severity.
- The effect of the crack on longitudinal frequency ratios intensively depends on the crack severity; by increasing the crack severity the frequency ratios are decreased.
- Surface density, has a decreasing effect on frequency ratios of nanorods. However, surface Lamé may have a decreasing or increasing effect on the frequency ratios of nanorods.
- For silicon nanorods, both surface energy and crack have decreasing effects. Meanwhile for aluminum nanorods, including surface Lamé parameters leads the frequency ratios to increase but including crack leads the frequency ratios to decrease.
- There is a crack severity value in which the increasing effect of surface energy and decreasing effect of crack, cancel out each other and consequently, the frequency remains unchanged.

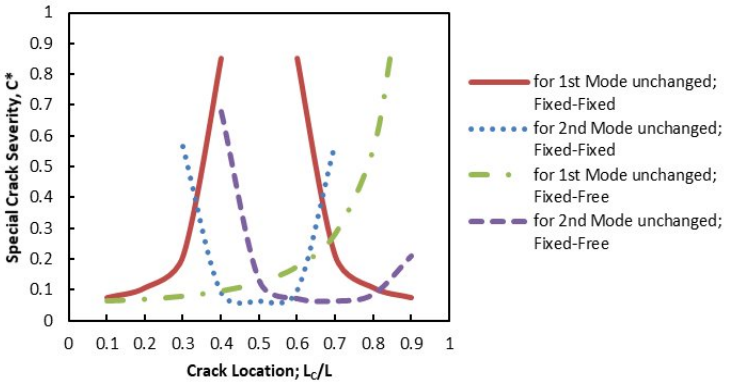

Fig.12
Special crack severity for unchanging the first and second longitudinal frequencies, for aluminum cracked nanorods with fixed-fixed and fixed-free boundary conditions for different crack locations.

REFERENCES

[1] Nowak A.S., Collins K.R., 2012, Reliability of structures, CRC Press.
[2] Grassian V.H., 2008, Nanoscience and Nanotechnology: Environmental and Health Impacts, Wiley.
[3] Klabunde K.J., 2001, Introduction to Nanotechnology, In Nanoscale Materials in Chemistry, https://doi.org/10.1002/0471220620.ch1.
[4] Wang M.F., Du G.J., Xia D.Y., 2013, Molecular dynamics simulation of microcrack healing in copper nano-plate, Key Engineering Materials, doi:10.4028/www.scientific.net/kem.531-532.454.
[5] Ding J., Wang L.S., Song K., Liu B., Huang X., 2017, Molecular dynamics simulation of crack propagation in single-crystal aluminum plate with central cracks, *Journal of Nanomaterials*, doi:10.1155/2017/5181206.
[6] Hu Z.L., Lee K., Li X.F., 2018, Crack in an elastic thin-film with surface effect, *International Journal of Engineering Science* 123:158-73.
[7] Loya J., López-Puente J., Zaera R., Fernández-Sáez J., 2009, Free transverse vibrations of cracked nanobeams using a nonlocal elasticity model, *Journal of Applied Physics* 105:044309.
[8] Safarabadi M., Mohammadi M., Farajpour A., Goodarzi M., 2015, Effect of surface energy on the vibration analysis of rotating nanobeam, *Journal of Solid Mechanics* 7:299-311.
[9] Rahmanian S., Hosseini Hashemi S., 2019, Bifurcation and chaos in size-dependent nems considering surface energy effect and intermolecular interactions, *Journal of Solid Mechanics* 11:341-60.
[10] Demir C., Mercan K., Numanoglu H.M., Civalek O., 2018, Bending response of nanobeams resting on elastic foundation, *Journal of Applied and Computational Mechanics* 4:105-14.
[11] Torabi K., Dastgerdi J.N., 2012, An analytical method for free vibration analysis of Timoshenko beam theory applied to cracked nanobeams using a nonlocal elasticity model, *Thin Solid Films* 520:6595-602.
[12] Ghadiri M., Soltanpour M., Yazdi A., Safi M., 2016, Studying the influence of surface effects on vibration behavior of size-dependent cracked FG Timoshenko nanobeam considering nonlocal elasticity and elastic foundation, *Applied Physics* A 122:520.
[13] Hosseini-Hashemi S., Fakher M., Nazemnezhad R., 2013, Surface effects on free vibration analysis of nanobeams using nonlocal elasticity: a comparison between Euler-Bernoulli and Timoshenko, *Journal of Solid Mechanics* 5:290-304.
[14] Numanoğlu H.M., Ersoy H., Akgöz B., Civalek Ö., 2022, A new eigenvalue problem solver for thermo-mechanical vibration of Timoshenko nanobeams by an innovative nonlocal finite element method, *Mathematical Methods in the Applied Sciences* 45:2592-614.
[15] Soltanpour M., Ghadiri M., Yazdi A., Safi M., 2017, Free transverse vibration analysis of size dependent Timoshenko FG cracked nanobeams resting on elastic medium, *Microsystem Technologies* 23:1813-30.
[16] Jalaei M.H., Thai H.T., Civalek □., 2022, On viscoelastic transient response of magnetically imperfect functionally graded nanobeams, *International Journal of Engineering Science* 172:103629.
[17] Roostai H., Haghpanahi M., 2014, Vibration of nanobeams of different boundary conditions with multiple cracks based on nonlocal elasticity theory, *Applied Mathematical Modelling* 38:1159-69.
[18] Karličić D., Jovanović D., Kozić P., Cajić M., 2015, Thermal and magnetic effects on the vibration of a cracked nanobeam embedded in an elastic medium, *Journal of Mechanics of Materials and Structures* 10:43-62.
[19] Khorshidi M.A., Shaat M., Abdelkefi A., Shariati M., 2017, Nonlocal modeling and buckling features of cracked nanobeams with von Karman nonlinearity, *Applied Physics* A 123:62.
[20] Hasheminejad S.M., Gheshlaghi B., Mirzaei Y., Abbasion S., 2011, Free transverse vibrations of cracked nanobeams with surface effects, *Thin Solid Films* 519:2477-82.
[21] Hosseini-Hashemi S., Fakher M., Nazemnezhad R., Haghighi M.H.S., 2014, Dynamic behavior of thin and thick cracked nanobeams incorporating surface effects, *Composites Part B: Engineering* 61:66-72.
[22] Wang K., Wang B., 2015, Timoshenko beam model for the vibration analysis of a cracked nanobeam with surface energy, *Journal of Vibration and Control* 21:2452-64.
[23] Hu K.M., Zhang W.M., Peng Z.K., Meng G., 2016, Transverse vibrations of mixed-mode cracked nanobeams with surface effect, *Journal of Vibration and Acoustics* 138:011020.
[24] Akbas S.D., 2016, Analytical solutions for static bending of edge cracked micro beams, *Structural Engineering and Mechanics* 59:579-99.
[25] Khorshidi M.A., Shariati M., 2017, Buckling and postbuckling of size-dependent cracked microbeams based on a modified couple stress theory, *Journal of Applied Mechanics and Technical Physics* 58:717-24.
[26] Khorshidi M.A., Shariati M., 2017, A multi-spring model for buckling analysis of cracked Timoshenko nanobeams based on modified couple stress theory, *Journal of Theoretical and Applied Mechanics* 55:1127-39.
[27] Beni Y.T., Jafaria A., Razavi H., 2014, Size effect on free transverse vibration of cracked nano-beams using couple stress theory, *International Journal of Engineering-Transactions B: Applications* 28:296-304.
[28] Sourki R., Hoseini S., 2016, Free vibration analysis of size-dependent cracked microbeam based on the modified couple stress theory, *Applied Physics A*. 122:413.
[29] Akbaş Ş.D., 2017, Free vibration of edge cracked functionally graded microscale beams based on the modified couple stress theory, *International Journal of Structural Stability and Dynamics* 17:1750033.
[30] Loya J., Aranda-Ruiz J., Fernández-Sáez J., 2014, Torsion of cracked nanorods using a nonlocal elasticity model, *Journal of Physics D: Applied Physics* 47:115304.

[31] Rahmani O., Hosseini S., Noroozi Moghaddam M., Fakhari Golpayegani I., 2015, Torsional vibration of cracked nanobeam based on nonlocal stress theory with various boundary conditions: an analytical study, *International Journal of Applied Mechanics* 7:1550036.
[32] Nazemnezhad R., Fahimi P., 2017, Free torsional vibration of cracked nanobeams incorporating surface energy effects, *Applied Mathematics and Mechanics* 38:217-30.
[33] Hsu J.C., Lee H.L., Chang W.J., 2011, Longitudinal vibration of cracked nanobeams using nonlocal elasticity theory, *Current Applied Physics* 11:1384-8.
[34] Yaylı M.Ö., Çerçevik A.E., 2015, Axial vibration analysis of cracked nanorods with arbitrary boundary conditions, *Journal of Vibroengineering* 17.
[35] Hosseini A.H., Rahmani O., Nikmehr M., Golpayegani I.F., 2016, Axial vibration of cracked nanorods embedded in elastic foundation based on a nonlocal elasticity model, *Sensor Letters* 14:1019-25.
[36] Rao S.S., 2007, Vibration of continuous systems, John Wiley & Sons.
[37] Gurtin M.E., Murdoch A.I., 1975, A continuum theory of elastic material surfaces, *Archive for Rational Mechanics and Analysis* 57:291-323.
[38] Nazemnezhad R., Shokrollahi H., 2019, Free axial vibration analysis of functionally graded nanorods using surface elasticity theory, *Modares Mechanical Engineering* 18:131-41.
[39] Nazemnezhad R., Shokrollahi H., 2020, Free axial vibration of cracked axially functionally graded nanoscale rods incorporating surface effect, *Steel and Composite Structures* 35:449-62.